Phycological Research

Phycological Research 2026; **74:** 8–21 doi: 10.1111/pre.70014

Multiple independent origins of asexuality and polyploidy among cryptic species of the brown alga *Scytosiphon promiscuus* (Scytosiphonaceae, Ectocarpales)

Masakazu Hoshino [1,2*] **Masanori Hiraoka** [3] **Kevin C. Wakeman,** [4] **Shimpei F. Hiruta** [5] **and Kazuhiro Kogame** [6]

[1]Research Center for Inland Seas, Kobe University, Kobe, Japan, [2]Department of Algal Development and Evolution, Max Planck Institute for Biology Tübingen, Tübingen, Germany, [3]Usa Marine Biological Institute, Kochi University, Tosa, Japan, [4]Institute for the Advancement of Higher Education, Hokkaido University, Sapporo, Japan, [5]The Mt. Fuji Institute for Nature and Biology, Showa Medical University, Fuji-Yoshida, Japan and [6]Department of Biological Sciences, Faculty of Science, Hokkaido University, Sapporo, Japan

SUMMARY

Although asexual populations and species have been frequently reported in seaweeds, their nature (e.g. origins and distribution patterns relative to closely related sexual counterparts) remains largely unknown. This is likely because determining the species identity, sex, and phase of individual organisms is often troublesome, making it difficult to comprehensively survey reproductive modes across many populations within a single species. In this study, we demonstrated that reduced-representation sequencing (RRS), a method of sequencing a fraction of the genome using high-throughput DNA sequencing platforms, is a simple and effective tool to investigate the reproductive modes of populations. To uncover the evolutionary trajectory of asexuals in *S. promiscuus*, which is known to include both sexual and asexual populations, we performed an RRS approach, MIG-seq. By applying MIG-seq to 122 individuals from 20 localities, mainly across Japan, we were able to: (i) estimate genetic diversity and phylogenetic relationships of populations; (ii) detect possible cryptic species (*spro1* and *spro2*); (iii) develop a pair of polymerase chain reaction-based sex markers to identify the sex and ploidy of individuals; and (iv) discover polyploid populations in *spro1* and female-dominant populations in *spro2*, both of which appear to be maintained asexually. By subsequently conducting crossing experiments and phylogenetic analysis using the mitochondrial gene *cox1* and nuclear gene *cetn-int2*, we confirmed that *spro1* and *spro2* are reproductively isolated. We also uncovered that polyploid populations have emerged multiple times in *spro1*, and one of these populations originated from hybridization between *S. promiscuus* and *S. shibazakiorum*, while the other populations originated from intraspecies crossing within *S. promiscuus*. It is surprising that multiple pathways to asexuality were found within such a narrow phylogenetic scope.

Key words: Allopolyploidy, autopolyploidy, Gametic incompatibility, linkage disequilibrium, MIG-seq, parthenogenesis, reproductive barrier, sex marker.

INTRODUCTION

There are numerous reports of macroalgal species/populations that reproduce solely by asexual reproduction, but little is known about their distribution patterns compared with those of their sexual relatives, states of sexual traits, or origin (e.g. Kamiya *et al*. 2017; Hoshino *et al*. 2021a, 2024). This is likely because comprehensive studies examining multiple populations of a specific species (e.g. Zupan and West 1988; West and Zuccarello 1999; Ardehed *et al*. 2016; Hiraoka and Higa 2016) remain scarce; many studies have reported the reproductive modes (sexual/obligate asexual) of individual populations (e.g. Müller 1977; Hiraoka *et al*. 2003). This scarcity is probably due to the difficulty and time-consuming nature of assessing the reproductive modes of macroalgal populations. Within a population, the presence of both male and female individuals is a good indicator that the population reproduces sexually. However, if the gametophyte generation is microscopic, the presence of male and female individuals can only be confirmed by culturing the meiospores from the sporophyte (e.g. Chordariaceae; Peters 1987). Even if the gametophytes are macroscopic, when they are immature, it is often impossible to determine their sex or even their generation (i.e. sporophyte or gametophyte) based on morphology alone (e.g. *Gracilaria* and *Dictyota*; Krueger-Hadfield *et al*. 2021; Arai *et al*. 2024). Even when they are mature, in isogamous taxa, it is impossible to distinguish the sexes morphologically, necessitating crossing experiments to identify sex (e.g. *Ulva* and *Scytosiphon*; Hiraoka and Higa 2016; Hoshino *et al*. 2019). Species complexes are often encountered that are morphologically indistinguishable and have overlapping distributions. In such cases, it is necessary to verify the species identity of the population using molecular data (Hoshino *et al*. 2021a). Investigating the reproductive modes of multiple populations is highly time-consuming.

Reduced-representation sequencing (RRS), which sequences a fraction of the genome using high-throughput DNA sequencing platforms (e.g. ddRAD-seq: Peterson *et al*. 2012), has become commonly used in population genetic studies because it generates a large number of single nucleotide polymorphisms (SNPs) at a relatively low cost. A single RRS dataset has the potential to explore the sex and generation of individuals (e.g. Krueger-Hadfield *et al*. 2021), as well as the genetic diversity, reproductive modes of

*To whom correspondence should be addressed.
Email: mhoshino@harbor.kobe-u.ac.jp
Received 28 April 2025; accepted 11 September 2025.

populations, and phylogenetic relationships between individuals or populations (Hoshino *et al*. 2021a). Therefore, RRS should be a suitable approach for investigating the reproductive mode of macroalgal populations. Among RRS approaches, the polymerase chain reaction (PCR)-based method, multiplexed inter simple sequence repeat (ISSR) genotyping by sequencing (MIG-seq: Suyama and Matsuki 2015), which amplifies the ISSR region via PCR and genotypes the amplicons, would be a suitable method for algae. In contrast to non-PCR-based RRS such as ddRAD-seq, MIG-seq does not require a large amount of high-quality genomic DNA (Suyama and Matsuki 2015), which is often troublesome to extract from algae.

Among macroalgae, the reproductive modes within the genus *Scytosiphon* could be better studied through MIG-seq technologies. *Scytosiphon* has a heteromorphic alternation of generations, with macroscopic dioicous gametophytes (haploid) that are morphologically indistinguishable between sexes, alternating with microscopic discoid sporophytes (diploid; Fig. 1a). They also possess a UV sex determination system (Barrera-Redondo *et al*. 2025), and their sexual reproduction is nearly isogamous: female gametes are slightly larger than male gametes. Female gametes settle on the substratum sooner than male gametes and secrete sex pheromones that attract male gametes (Fu *et al*. 2014; Fig. 1a). Five *Scytosiphon* species, which are morphologically almost indistinguishable but are reproductively isolated, are known around Japan (Hoshino *et al*. 2021b). Among them, *S. promiscuus* McDevit & G.W. Saunders and *S. lomentaria* (Lyngbye) Link are known to have parthenogenetic populations consisting of only females (referred to as Amazon populations, after the female-only warrior tribe in Greek mythology; Hoshino *et al*. 2024), in addition to populations consisting of both male and female gametophytes (sexual Hoshino *et al*. 2021a, 2024). In *S. lomentaria*, the geographical distribution patterns and phylogenetic relationships of sexual and Amazon populations have been well studied (Hoshino *et al*. 2021a). In *S. promiscuus*, despite its worldwide distribution similar to *S. lomentaria* (Hoshino *et al*. 2021b), only a few populations have been studied (Croce *et al*. 2023; Hoshino *et al*. 2024), and the nature of their asexual lineages has not been characterized.

In the present study, we used MIG-seq data to investigate the reproductive mode of *S. promiscuus* populations within Japan and Far East Russia with the aims to use RRS data to (i) investigate the genetic diversity and phylogenetic relationships across populations, (ii) delineate cryptic species, and (iii) develop sex markers for accelerating the identification of sex and ploidy.

MATERIALS AND METHODS

SNPs calling and filtering

We analyzed the previously generated MIG-seq data of 122 individuals collected in Japan and Far East Russia (Fig. 2; Croce *et al*. 2023). These individuals were identified as *S. promiscuus* in our previous study by examining the partial sequence of the mitochondrial gene *cox*1 (Hoshino

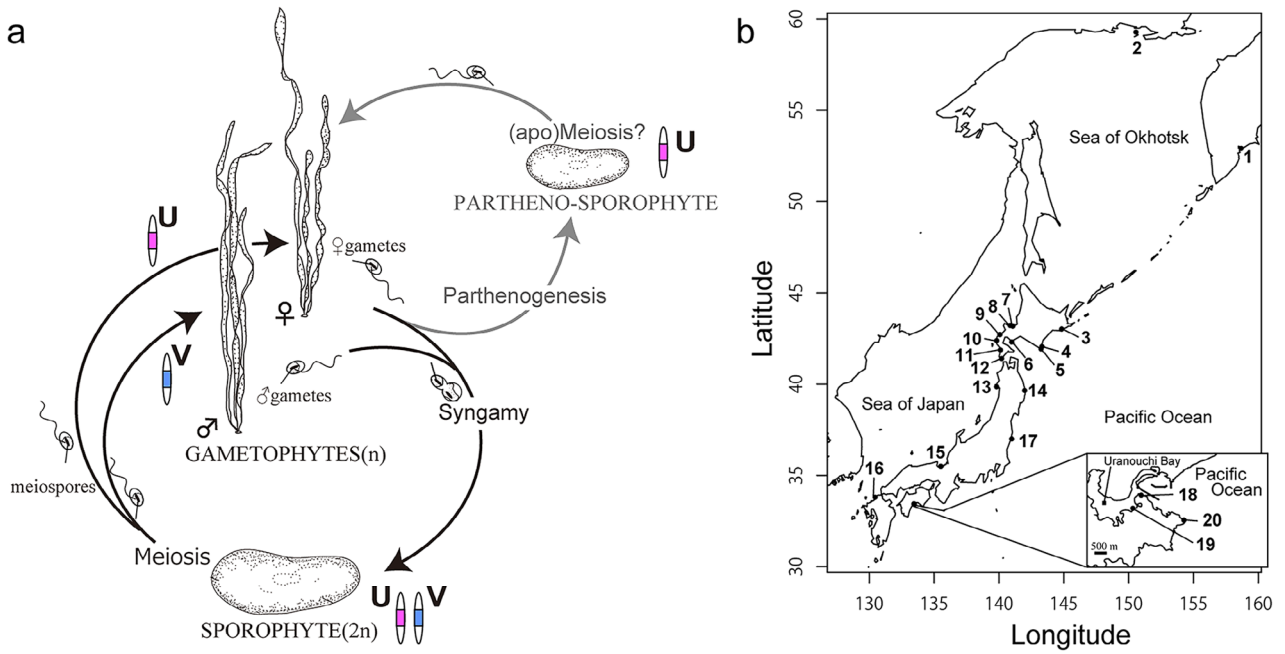

Fig. 1. (a) Life cycle of *Scytosiphon*. The sexual life cycle is indicated by the black arrows. Gametophytes are dioicous and isomorphic. Male and female gametes are almost identical in terms of size. Sex is determined at meiosis, depending on whether meiospores inherit a female (U) or male (V) chromosome. The asexual life cycle, reported from Amazon populations (female parthenogenetic populations), is indicated by the gray arrows. Unfertilized female gametes develop into partheno-sporophytes. The figure is based on Hoshino (2021). (b) A map showing the sampling locations around Japan, with locality codes represented by Arabic numerals.

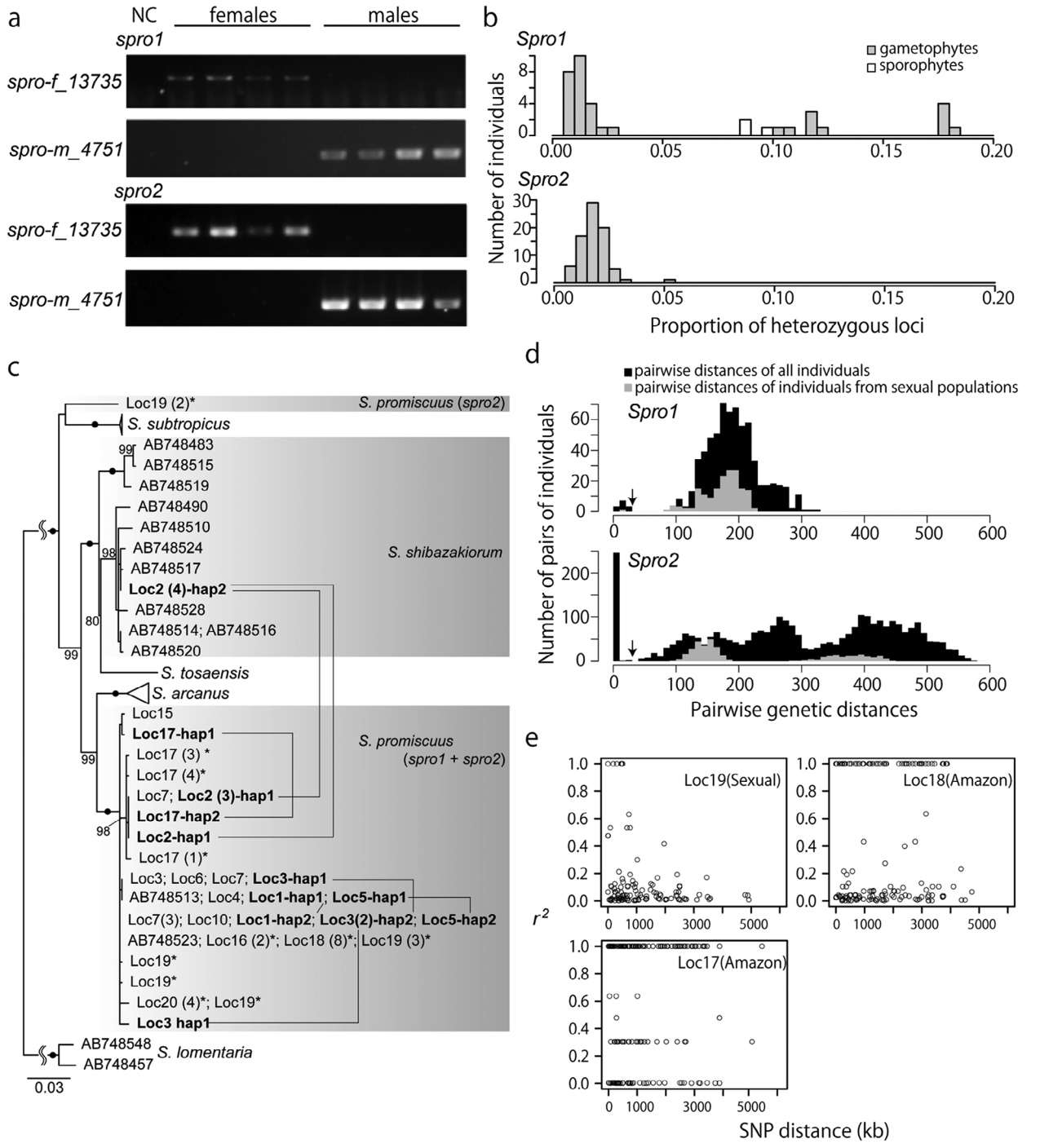

Fig. 2. (a) PCR results of PCR-based sex markers in female and male gametophytes. Specimen code of each gametophyte is shown in Fig. S2. (b) Histograms showing the proportion of heterozygous loci. Gametophytic individuals are indicated in gray, while sporophytic individuals are indicated in white. (c) Maximum likelihood tree based on *cetn*-int2 showing the phylogenetic position of haplotypes from polyploids. Haplotypes derived from individuals collected at the sampling locations shown in Fig. 1b are labeled with locality codes (Loc#), the number of individuals possessing the haplotype in parentheses, and haplotype codes (hap1 or hap2, if applicable). Haplotypes derived from polyploid gametophytes are shown in bold, those from spro2 individuals are marked with asterisks, and haplotypes originating from the same individual are connected by black lines. Only bootstrap values > 80 are shown. and the black circles indicate branches with full support (100). Scale bar = number of nucleotide substitutions per nucleotide site. (d) Histograms showing pairwise genetic distances. Pairwise distances of individuals from sexual populations (populations including both male and female individuals) are indicated in gray. The threshold distance (30) to recognize clonal lineages is indicated by arrows. (e) LD decay for one sexual population (locality 19) and two parthenogenetic Amazon populations (locality 17 and 18) of *spro2*. LD decay estimated for all scaffolds is shown in a single plot, as only a few LD values were calculated for each scaffold.

et al. 2018, 2021b). Morphologically, three individuals were sporophytes (i.e. discoid thalli), but all other individuals were gametophytes (i.e. erect thalli; Supplemental Table S1). The data from 39 individuals were newly analyzed in this study, while all other data had been analyzed in our previous study to investigate the phylogenetic relationships between Argentinean and Japanese populations (Croce *et al*. 2023). All data have been deposited in the NCBI database (BioProject accession no.: PRJNA887098).

The raw reads were paired-end: read 1 sequences are 80 bp and read 2 sequences are 94 bp. The first 14 bp of read 2 sequences, which are ISSR primer and anchor sequences (Suyama and Matsuki 2015), were trimmed using the program 'fastx_trimmer' in FASTX-Toolkit v0.0.14 (http://hannonlab.cshl.edu/fastx_toolkit). Subsequently, primer sequences (Suyama and Matsuki 2015) and low-quality reads were removed using Trimmomatic v0.39 (Bolger *et al*. 2014) with the following parameters: SLIDINGWINDOW:4:15 LEADING:25 TRAILING:25 MINLEN:50. The quality-filtered reads were mapped to a reference genome using BWA v0.7.17 with the BWA-MEM algorithm (Li and Durbin 2009). As the reference genome, a genome of the female gametophyte of *S. promiscuus*, which was assembled in Hoshino *et al*. (2024), was used. The resulting *sam* files were converted to *bam* files and sorted by coordinates using Samtools v1.6 (Li *et al*. 2009). The mapping rate of each individual was monitored using BamTools v2.5.2 (Barnett *et al*. 2011). To call SNPs, the sorted *bam* files were analyzed by the Stacks v2.65 (Rochette *et al*. 2019) pipeline, ref_map.pl, with the default parameters, and only the first SNP was extracted from each locus. The resulting SNP datasets were then filtered by PLINK v2.00 (Chang *et al*. 2015). SNPs with missing rates exceeding 0.35 were firstly removed (*--geno 0.35*). Then, individuals with missing rates exceeding 0.45 and SNPs with allele frequency below 0.01 were removed (*--mind 0.45* and *--maf 0.01*). Finally, SNPs were thinned (*--bp-space 100*) so that no two SNPs are within 100 bp from one another. The filtered SNP dataset consisted of 115 individuals with 903 SNPs (*sproALL* dataset: genotyping rate = 0.80). *Scytosiphon promiscuus* was shown to consist of two cryptic species, *spro1* and *spro2* (see Results), and probably because of this, it was difficult to call the common SNPs between them. Thus, the SNP dataset from the Stacks pipeline was divided by each species and independently filtered by PLINK as described above. The resulting filtered SNP dataset of *spro1* consisted of 38 individuals with 668 SNPs (*spro1* dataset: genotyping rate = 0.83), and the dataset of *spro2* consisted of 79 individuals with 890 SNPs (*spro2* dataset: genotyping rate = 0.84). The number of shared and unique SNPs among the three datasets is given in Supplemental Fig. S1. All datasets were kept in diploid format as originally output by the Stacks pipeline, since they included possible polyploids and sporophytes along with haploid gametophytes. The format of the datasets was converted using PGDSpider v2.1.1.5 (Lischer and Excoffier 2012) for subsequent analyses.

Development of new PCR-based sex markers

PCR-based sex markers (i.e. PCR markers designed on non-recombining regions of sex chromosomes) are a powerful tool to identify the sex and generation of organisms with UV sex determination systems (Krueger-Hadfield *et al*. 2021; Arai *et al*. 2024). Thus, we examined whether sex markers can be developed from the MIG-seq data, although one pair of PCR-based sex markers has already been available in *Scytosiphon* (Hoshino *et al*. 2019). At first, reads after the quality control were analyzed by the Stacks pipeline, denovo_map.pl., for de novo assembly because the reference-guided pipeline (ref_map.pl) discards unmapped reads (i.e. reads from the sex-specific region of the male chromosome will be discarded as we used a female genome as the reference). One of the out files from the pipeline, 'populations.haplotypes.tsv', provided genotypes of individuals at each locus, indicating which locus was (was not) assembled in each individual. Loci of the sex-specific regions of sex chromosomes are expected to be assembled exclusively in one sex. Thus, among the individuals with known sex (34 females and 16 males; Supplemental Table S1), contigs that were assembled in only one sex—specifically in 10 or more females or five or more males—were treated as candidate sex-linked loci. From these candidate loci, two candidate female-linked and two candidate male-linked loci (Supplemental Table S2) were PCR-amplified to evaluate their potential as PCR-based sex markers. The primers were designed using Primer3 v0.4.0 (Untergasser *et al*. 2012) or manually (Supplemental Table S2). Template DNA for PCR was extracted from four male and four female individuals of both *spro1* and *spro2*, as previously (Hoshino *et al*. 2020). PCR was performed using KOD One® PCR Master-Mix (TOYOBO, Osaka, Japan) and TaKaRa PCR Thermal Cycler Dice (Takara Bio, Kusatsu, Japan). The PCR program consisted of a denaturation step at 98°C for 5 s, followed by 30 cycles of 98°C for 10 s, 60°C for 5 s, and 68°C for 1 or 2 s. The presence or absence of PCR products was checked by 1% agarose gel electrophoresis. The developed sex markers were used to examine the sex of individuals, and the identified sex was compared with those identified by crossing experiments and/or previously developed sex markers (Hoshino *et al*. 2019).

Detecting polyploid gametophytes and their sexuality

Our previous study identified putative polyploid gametophytes in *S. lomentaria*, which, despite being morphologically gametophyte, exhibited numerous heterozygous loci and amplification of both sex markers (Hoshino *et al*. 2021a). To determine if polyploids exist in *S. promiscuus*, we examined the number of observed homozygous loci and genotyped loci (non-missing loci) in each individual using PLINK by the flag '*--het*', and calculated the proportion of heterozygous loci for each individual. For individuals exhibiting a high proportion of heterozygous loci, we conducted sex-check PCR using the sex markers developed above, in addition to the previously developed sex markers (Hoshino *et al*. 2019).

For a part of individuals possessing both sex markers, the second intron region of the nuclear-encoded single-copy gene *centrin* (*cetn*-int2), which has been used in *Scytosiphon* species from Japan (Kogame *et al*. 2015; Hoshino *et al*. 2018), was sequenced to investigate the possible origins of their maternal and paternal genomes. Because the direct sequence

result was heterogeneous, probably due to overlapping sequences of maternal and paternal haplotypes, the PCR product was cloned using TArget Clone™ -Plus- (TOYOBO, Osaka, Japan) according to the manufacturer's instructions. For each individual, 8–16 colonies were used for colony PCR, and the amplicons were sequenced. Considering inter-clone variation due to PCR errors, identical sequences obtained from at least two colonies were recognized as the true sequences. The obtained *cetn*-int2 sequences were aligned with those retrieved from GenBank using MAFFT in GUIDANCE2 Server (Landan and Graur 2008; Penn *et al*. 2010; Sela *et al*. 2015), and the positions in the alignments with a score below 0.93 (i.e. poorly aligned positions) were excluded. The resulting alignment was analyzed using IQ-TREE v2.2.2.7 (Chernomor *et al*. 2016; Kalyaanamoorthy *et al*. 2017; Minh *et al*. 2020) for maximum likelihood (ML) analysis. The ML analysis by IQ-TREE was performed with 1,000 standard nonparametric bootstrap replicates and with the best nucleotide models inferred by the flag '*-m MFP*'.

For the *S. promiscuus* (*spro1*) population at locality 3 (Fig. 1), where possible polyploid gametophytes were newly detected, we conducted another sampling for crossing experiments to examine the sexuality of such polyploid gametophytes. The collected gametophytes were kept in a cooled container and transferred to the lab. Release of zoids was then induced as described in Han *et al*. (2014). For the 12 individuals that released zoids, we mixed zoids from 3 to 4 individuals under a microscope to examine whether fertilization occurred. For the 30 individuals, including those that released zoids, we performed *cox*1 sequencing (Kogame *et al*. 2015) and sex-check PCR to confirm that these newly collected gametophytes belong to *spro1* and are polyploid.

Clonal diversity of populations

To examine clonal diversity of each population, the number of clonal lineages in each dataset (*spro1* and *spro2*) was assessed using '*assign clone*' function of GenoDive v3.04 (Meirmans and Van Tienderen 2004; Meirmans 2020), following previous work (Hoshino *et al*. 2021a). This function works by first calculating a matrix of genetic distances and then choosing a threshold distance. If the distance between a pair of individuals is below a user-defined threshold, they are deemed to belong to the same clonal lineage (Meirmans 2020). We calculated a matrix of genetic distances using an infinite allele model with the default setting and determined the threshold distance (see details in Results). Each clonal lineage recognized here was treated as a single genotype, and Nei's genetic diversity corrected for samples size (*Div*; Nei 1987) and the clonal diversity index *R* (Dorken and Eckert 2001) were calculated in each population. *Div* was calculated by the '*clonal diversity*' function of GenoDive based on the equation: $Div = N\sum G_i^2/(N-1)$, where G_i is the frequency of the *i*th genotype and *N* is the total number of sampled individuals. While, the second index *R* was calculated by the equation: $R = (G\text{-}1)/(N\text{-}1)$, where *G* is the number of distinct genotypes and *N* is the total number of sampled individuals.

Linkage disequilibrium

Since recombination should be absent in parthenogens, linkage disequilibrium (LD) is expected to be higher in parthenogenetic populations compared with sexual populations, where sexual reproduction (recombination) decreases LD (Freitas *et al*. 2023). To test this expectation, the LD coefficient r^2 value was calculated in one sexual and two parthenogenetic Amazon populations of *S. promiscuus*, *spro2* (locality 17–19; Fig. 1b), where MIG-seq data was available for relatively many individuals (21–24 individuals per population, after filtering). Because we did not detect any polyploid individuals in the *spro2* dataset, heterozygous loci in the dataset were considered to have come from sequencing or mapping error. Thus, these heterozygous loci were excluded from the dataset using a filtering function of TASSEL v5.2.93 (Bradbury *et al*. 2007), and then the r^2 value was calculated in each population using vcftools v0.1.16 (Danecek *et al*. 2011) by the flag '*--hap-r2*.' The calculated r^2 values were visualized as an LD decay plot using R software.

Population genetic structure and phylogeny

To infer the population genetic structure and the phylogeny among individuals, we performed a clustering analysis and maximum likelihood (ML) analysis for the *sproALL* dataset. For the clustering analysis, we used STRUCTURE v2.3.4 (Pritchard *et al*. 2000). The number of clusters (*K*) of 1–8 was tested by running 10 simulations for each *K*, with 100,000 Markov chain Monte Carlo (MCMC) steps and a burn-in of 100,000, using the model with admixture and correlated allele frequencies. Calculation of mean log probability of data for each *K*, L(*K*), and ΔK values (Evanno *et al*. 2005) and visualization of the outputs were performed using the R package pophelper v2.3.1 (Francis 2017). For the ML analysis, 67 invariant sites were excluded from the dataset using the ascbias.py script (https://github.com/btmartin721/raxml_ascbias). The ML analyses were performed using IQ-TREE v2.2.0.3 with 1,000 ultrafast bootstrap pseudoreplicates and 1,000 bootstrap pseudoreplicates for the SH-like approximate likelihood ratio test (SH-aLRT; Guindon *et al*. 2010); best-fit models were inferred by the flag '*-m MFP + ASC*.' The resulting trees were visualized using Figtree v1.4.3 (http://tree.bio.ed.ac.uk/software/figtree/).

Species delimitation

As the genome-wide SNP analyses showed, *S. promiscuus* consists of two distinct genetic groups, *spro1* and *spro2*; we examined if these two entities are the same species or not. We firstly performed species delimitation analyses based on the mitochondrial gene *cox*1, which is the widely used to assess species diversity of brown algae (Leliaert *et al*. 2014), including *Scytosiphon* (Hoshino *et al*. 2021b). PCR and sequencing of *cox*1 were conducted as in Kogame *et al*. (2015). Newly obtained sequences [110 sequences of *cox*1 (−617 bp): LC846453–LC846556, LC888467–LC888472] were aligned with the *cox*1 sequences of other *Scytosiphon* species and their related genera (Table S1) using MAFFT v7.525 (Katoh 2002; Katoh and Standley 2013). The alignment was manually trimmed to 600 bp, and redundant

identical sequences were excluded using CD-hit v4.8.1 (Li and Godzik 2006). Using the resulting alignment (139 OTUs), we performed three different species delimitation analyses: Generalized Mixed Yule Coalescent (GMYC) (Pons *et al*. 2006; Fujisawa and Barraclough 2013), poisson tree processes (PTP) (Zhang *et al*. 2013), and assemble species by automatic partitioning (ASAP) (Puillandre *et al*. 2021). The first two methods are model-based species delimitation analyses, and the last one is a barcode gap-based analysis. For GMYC, ultrametric trees were built using BEAST v2.6.3 (Bouckaert *et al*. 2019) with the substitution model of TN93 + G + I (the best model inferred by MEGA v7; Kumer *et al*. 2016), MCMC steps of 50,000,000, and four different combinations of tree branching pattern models (Yule model or coalescent model) and molecular evolution models (strict clock model or relaxed clock model). Each BEAST run was summarized to a maximum clade credibility tree using TreeAnnotator with a burn-in of 50%, and the resulting tree was used for single threshold GMYC by the R package Splits. Additionally, *p*-distances among putative species, inferred by GMYC with coalescent and relaxed clock model priors, were calculated using MEGA. For PTP, a ML tree was constructed using IQ-tree with 1,000 nonparametric bootstrap and the best substitution models inferred by the flag '*-m MFP*', and the constructed tree was used for PTP analysis implemented in iTaxoTools (Vences *et al*. 2021). For ASAP, the *cox*1 alignment was analyzed using ASAP software implemented in iTaxoTools with the substitution model of K80. ASAP automatically determines multiple barcode gaps from a given alignment, partitions the alignment into putative species based on each barcode gap, and assigns an ASAP score to each partitioning (lower scores indicating better partitioning; Puillandre *et al*. 2021). As a result of ASAP, we selected the partitioning with the best ASAP score from those with barcode gaps ranging from 0.01 to 0.05.

In addition to the *cox*1-based species delimitation analyses, we carried out crossing experiments between *spro1* and *spro2* individuals from locality 16. Culture strains of gametophytes, which were previously established (Kogame *et al*. 2015; Hoshino *et al*. 2024), were maintained using plastic Petri dishes (90 × 20 mm) with PESI medium (Tatewaki 1966), at 10°C short-day (SD: 8:16 h, light:dark) condition with fluorescent light of 30–50 μmol m^{-2} s^{-1} photon flux density. To quantify the fertilization rate, a Fuchs-Rosenthal hemocytometer (WATSON Co. Ltd., Tokyo, Japan) was used. A suspension of female gametes was loaded into the hemocytometer and incubated for several minutes at 10°C to allow the gametes to settle. Unsettled gametes were then washed away by adding an excess amount of medium. After counting the number of settled gametes under an inverted light microscope (CKX53; Olympus, Hachioji, Japan), a suspension of male gametes was added to the hemocytometer. Following an incubation of at least 1 h at 10°C, the number of zygotes (i.e. cells with more than one eyespot) was examined under an inverted light microscope.

RESULTS

New PCR-based sex markers

One pair of sex markers was successfully developed (Fig. 2a; Table 1). From the de novo assembled contigs, 40 putative female-linked and 26 putative male-linked loci were identified. Among the four candidate sex-linked loci used for PCR (two for each sex), one was amplified in a female-specific manner, and the other one was amplified in a male-specific manner (Fig. 2a). The amplicon size of the female marker was greater than 3 kb in *spro1* females, but around 200 bp in *spro2* females (Supplemental Fig. S2). Meanwhile, the amplicon size of the male marker was around 400 bp in both *spro1* and *spro2* males (Supplemental Fig. S2). We also examined in which individuals the contigs used as sex markers were assembled. The contig of the female marker was assembled only in some *spro2* females, while that of the male marker was assembled only in some males, polyploids (see below results), and sporophytes of *spro1*, indicating the difficulty of identifying the sex of individuals solely from the presence or absence of the assembled contigs (Table 2).

Sex identification using the new sex markers was consistent with those identified by crossing experiments and/or previously reported sex markers (Hoshino *et al*. 2019), with the exception of four individuals from locality 3 and two individuals from locality 13. For these six individuals, the new female marker was not amplified, but the previously reported female marker was amplified (Supplemental Table S1).

Polyploid gametophytes

Heterozygous loci were observed in all individuals, including those expected to be haploid, suggesting that some of the observed heterozygosity may result from sequencing or mapping errors. The proportion of heterozygous loci observed in each individual was less than 5% in most cases (Fig. 2b). The *spro1* dataset included three sporophytes, and their heterozygous loci proportions ranged from 8.6% to 9.8% (Fig. 2b), indicating the heterozygosity level of true diploids. Apart from the sporophytes, 11 individuals of *spro1* and one individual of *spro2* exhibited heterozygous loci exceeding 5% (Fig. 2b). Using the newly developed PCR-based sex marker to verify the sex of these 12 individuals, both male and female markers were amplified in the 11 individuals from *spro1* (locality 1–3, 5, 17), indicating that they are polyploid gametophytes (at least diploid). Cloning of *cetn*-int2 for the *spro1* polyploid gametophytes showed that they have two haplotypes. Phylogenetic analysis revealed that both haplotypes of the *spro1*

Table 1. Newly developed PCR-based sex markers.

Sex specificity	Name	Forward primer sequence	Reverse primer sequence	Approx. PCR product size
Female marker	spro-f_13735	GGTTGTCCCTTTTCCCCAAA	CTCGCTGCTACTGTACCCTT	200 bp in *spro1*, but >3 kb in *spro2*
Male marker	spro-m_4751	AGGGTTCATCAAATAGGGGCT	CCTTCGAACCTTTGCTTCTGG	350 bp

Table 2. Reproductive mode, genetic diversity, and sex ratio of each locality.

Locality code	Mode of reproduction	n. individuals (MIG-seq individuals)	n. clonal lineages	Identity of assigned clonal lineages	*Div*	*R*	Sex ratio based on crossing experiments and/or PCR-based sex markers	Expected sex ratio from MIG-seq data
spro1							f:m:fm:NA	f:m:fm:NA
2	Asexual polyploids	4	1	c19 (4)	0.000	0.00	0:0:4:0	0:0:0:4
3	Asexual polyploids	4	1	c1 (4)	0.000	0.00	0:0:4:0	0:3:0:1
6	Sexual	3	3	c12–c14	1.000	1.00	2:1:0:0	0:1:0:2
7	Sexual	3	3	c2–c4	1.000	1.00	2:1:0:0	0:0:0:3
8	Sexual	5 (3 sporophytes)	4	c20, c21, c22 (2), c23	0.900	0.75	1:1:3:0	0:3:0:2
13	?	2	2	c29, c30	1.000	1.00	2:0:0:0	0:0:0:2
15	Sexual	4	4	c15–c18	1.000	1.00	2:2:0:0	0:2:0:2
16	Sexual	4	4	c7–c10	1.000	1.00	1:3:0:0	0:0:0:4
spro2								
16	Sexual	6	6	C26–C31	1.000	1.00	5:1:0:0	3:0:0:3
17	Parthenogenetic Amazon	23	9	C2, C32 (3), C33 (5), C34 (3), C35 (3), C36, C37 (5), C38, C39	0.885	0.36	23:0:0:0	13:0:0:10
18	Parthenogenetic Amazon	24	4	C1 (21), C2–C4	0.239	0.13	24:0:0:0	22:0:0:2
19	Sexual	21	21	C5–C25	1.000	1.00	14:10:0:0	8:0:0:13
20	Parthenogenetic Amazon	5	2	C3 (4), C40	0.400	0.25	5:0:0:0	4:0:0:1

Only localities where multiple individuals were collected are shown. Clone codes (c##) are given to each clonal lineage. For clonal lineages that were found in multiple individuals in one population, the number of individuals is shown in parentheses. *Div*, Nei's genetic diversity corrected for sample size; *R*, clonal diversity index. Two types of sex ratios are shown: the one inferred by crossing experiments and/or PCR-based sex markers, and the other one is based on the presence or absence of sex-linked MIG-seq assemblies. f, the number of females; m, the number of males; fm, the number of individuals having both female and male markers from PCR amplification/MIG-seq assemblies; NA, not available. The population at locality 13 appears to be genetically sexual, but since no male individuals were observed, its reproductive mode was left undetermined (?).

polyploids from localities 1, 3, 5, and 17 belonged to the *S. promiscuus* clade (Fig. 2c). Meanwhile, *spro1* polyploids from locality 2 had one haplotype belonging to the *S. shibazakiorum* M.Hoshino & Kogame clade and another to the *S. promiscuus* clade (Fig. 2c), indicating that they are hybrids of *S. shibazakiorum* and *S. promiscuus*.

To examine the sexuality of *spro1* polyploid gametophytes at locality 3, 30 gametophytes were newly collected. Based on *cox*1 sequence, all individuals were identified as *S. promiscuus* (*spro1*), except one individual of *S. shibazakiorum* (Supplemental Table S1, sample code: Aikappu240415_1–5). Sex-check PCR for the 29 *spro1* individuals revealed that 19 had both male and female markers, 10 had only the female marker, and none had only the male marker (Supplemental Table S1). Among the 12 individuals used for the crossing experiments, 8 had both markers, and 4 had only the female marker. No fertilization was observed among them, suggesting that polyploids and females at locality 3 reproduce asexually.

Clonal diversity and reproductive mode of populations

The calculation of pairwise genetic distances showed that the distances among individuals from populations that are already known to include both males and females were typically greater than 100 (Fig. 2d). Furthermore, the histograms of the genetic distances showed a clear gap around 30–80 in *spro1* and 30–40 in *spro2*. Thus, a threshold distance of 30 was set to distinguish whether pairs of individuals belonged to the same clonal lineage (arrows in Fig. 2d). Using this threshold, the '*assign clone*' function of GenoDive identified 31 clonal lineages among 38 individuals in *spro1*, and 40 clonal lineages among 79 individuals in *spro2*. In populations where both male and female individuals were found (sexual populations), all individuals were usually assigned to different clonal lineages, resulting in both Nei's genetic diversity (*Div*) and the clonal diversity index (*R*) being close to 1 (Table 2). In contrast, in the two *spro1* populations where multiple polyploids were found (locality 2 and 3), and in the three *spro2* populations where only females were found (locality 17, 18, 20), individuals belonging to the same clonal lineage were observed, resulting in low genetic and clonal diversity (Table 2). These results suggest that the *spro1* polyploid populations and the *spro2* Amazon populations are both maintained asexually.

Low recombination rate in Amazon populations

As expected, in the sexual population at locality 19, the r^2 values tended to approach zero as the distance between SNPs increased (Fig. 2e). However, in the Amazon populations at locality 17 and 18, this tendency was not observed, and

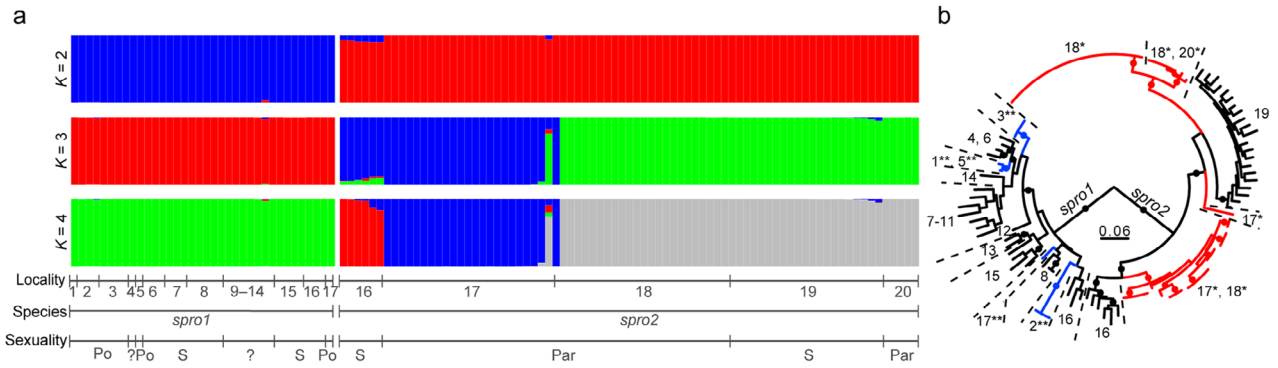

Fig. 3. (a) Result of the clustering analysis by STRUCTURE for $K = 2$, 3, and 4. The locality code, species identity, and sexuality (Po, polyploids; s, sexuals; Par, parthenogenic Amazons) of each individual is indicated below the plots. (b) Maximum likelihood tree based on MIG-seq data (836 SNPs). Full support (bootstrap value of 100) is indicated by a circle on the branches. The lineages of polyploid populations (double asterisk) are indicated by blue, while those of parthenogenetic Amazon populations (single asterisk) are shown in red color. Locality codes are given at the tips of external branches.

complete linkage (i.e. $r^2 = 1$) was frequently observed even between distant SNPs, demonstrating a low recombination rate (Fig. 2e).

Population structure and phylogeny inferred from SNPs

Both clustering and phylogenetic analyses inferred two distinct genetic groups in *S. promiscuus*: *spro1* and *spro2* (Fig. 3). In the STRUCTURE analysis, the ideal number of clusters (K) determined based on ΔK values was two (Fig. S3a), separating *spro1* and *spro2* (Fig. 3a). The two entities coexisted at localities 16 and 17, and the *spro2* individuals there, specifically the ones from locality 16, showed a slight admixture pattern. The mean L(K) values tended to increase with higher K but reached a plateau around $K = 4$ (Fig. S3b). The admixture pattern observed in *spro2* individuals from locality 16 at $K = 2$ disappeared when a greater number of clusters was assumed, while the distinctness between *spro1* and *spro2* was maintained (Fig. 3a). The phylogenetic analysis also supported the distinctness of *spro1* and *spro2* (Fig. 3b). Amazon populations (localities 17, 18, 20) were belonged to *spro2* and were polyphyletic. Meanwhile, polyploids from localities 1–3, 5, 17 belonged to *spro1* and were also polyphyletic. For the Amazon populations, external branches were extremely short compared with those of sexual populations (localities 16 and 19), indicating the genetic homogeneity of the individuals. Such short external branches were also observed in the polyploid populations at localities 2 and 3.

Two biological species in *S. promiscuus*?

The *p*-distance of *cox*1 between *spro1* and *spro2* was 0.0167–0.0250 (avg. = 0.0183). Among the three *cox*1-based species delimitation analyses, ASAP inferred the fewest species (8), did not distinguish between *spro1* and *spro2*, and the inferred species boundaries were consistent with those of the currently accepted six species (Fig. 4). Meanwhile, GMYC and PTP inferred more species (14–20). Only GMYC recognized *spro2* as a distinct species (Sp-G2) regardless of the prior setting, but also divided *spro1* into at least two species (Sp-G1, G3; Fig. 4).

Crossing experiments indicated that *spro1* and *spro2* at locality 16 are reproductively isolated due to gametic incompatibility. In intra-'species' crossing, male gametes attached to female gametes via their anterior flagella and subsequently underwent zygote formation. The fertilization rate was 84.4% in *spro1* and 74.6–91.1% in *spro2* (Table S3). In contrast, in inter-'species' crossing, the attachment of male gametes to female gametes via the anterior flagella was only temporary, and the male gametes eventually swarmed away from female gametes (Supplemental Movie S1). No instance of zygote formation was observed in inter-'species' crossings, and almost no zygotes (i.e. cells showing more than one eyespot) were detected during counting, resulting in a fertilization rate of 0–0.5% (Table S3).

DISCUSSION

Identification of sex, generation, and ploidy

Sex and ploidy (or phase) are crucial pieces of information for understanding the reproductive modes and demography of populations, but their identification is often challenging in seaweeds (Krueger-Hadfield 2024). In recent years, seaweeds with a UV sex determination system (e.g. Fig. 1a) have been studied using non-recombining regions of sex chromosomes as PCR markers to efficiently identify sex and phase (e.g. Couceiro *et al*. 2015; Lipinska *et al*. 2015; Hoshino *et al*. 2019; Krueger-Hadfield *et al*. 2021; Arai *et al*. 2024). In these cases, sex-specific PCR markers have been developed using whole-genome sequencing data, transcriptome data, ddRAD-seq data, or a combination of these approaches. In this study, we developed a pair of sex markers using MIG-seq data. Although our female marker did not work for some *spro1* individuals from localities 3 and 13, both sex markers usually performed well for *S. promiscuus*, allowing identification of sex, generations, and ploidy of the individuals. A more

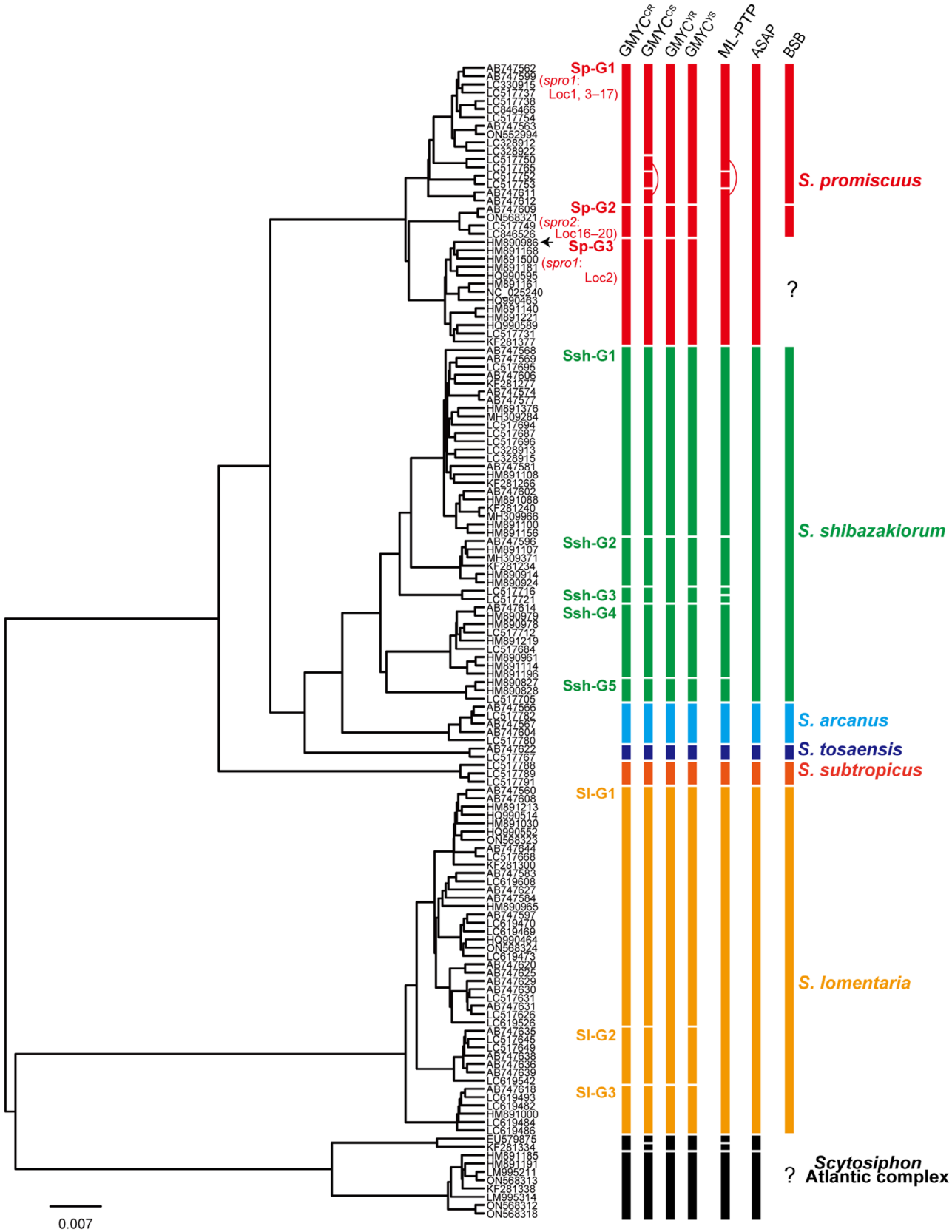

Fig. 4. Legend on next page.

universal female marker could potentially be developed by sequencing the female marker in many individuals and designing new primers in conserved regions or by examining other putative female-linked contigs.

We expected that the sex and ploidy of each individual could be inferred without performing PCR, simply by checking for the presence or absence of assembled sex-linked contigs (i.e. the contigs used as the PCR-based sex markers). However, this did not work. The contig used as the male marker did not assemble in *spro2* males, and the contig used as the female marker was not assembled in *spro1* females. In other words, these contigs were amplified by PCR but were completely absent in assembly data in a species-specific manner. This is likely due to the library preparation strategy of MIG-seq. MIG-seq library utilizes size-selected amplicons (300–800 bp) of PCR using primers targeting SSR regions. The female marker was more than 3 kb in *spro2*, and thus, this would have been excluded during the size selection even if it was amplified in *spro2* individuals. Furthermore, because SSR regions rapidly evolve (Ellegren 2004), they might not be conserved enough between *spro1* and *spro2* to have common amplicons, even if ISSR regions were conserved between the two species.

Polyploids

Polyploids, which are morphologically gametophyte but possess two sets of genomes, have independently emerged multiple times in *S. promiscuus*. Except for those in locality 2, which are allopolyploids with genomes from different species, all others were identified as autopolyploids with genomes from the same species. The autopolyploids likely arose from intraspecific crosses within *S. promiscuus*, while the allopolyploids are interspecific hybrids between *S. promiscuus* and *S. shibazakiorum*. Autopolyploids have also been reported in *S. lomentaria* (Hoshino *et al*. 2021a), but this is the first example of interspecies hybrid polyploids (allopolyploids) in *Scytosiphon*. In brown algae, it is likely the third known case of natural allopolyploids, following *Pelvetiopsis hybrida* Neiva, J., Raimondi, P.T., Pearson, G.A., Serrão, E.A., and *P. limitata* (Setchell) N.L. Gardner (Neiva *et al*. 2017; Sousa *et al*. 2019). In land plants and animals, polyploidization is well known as a trigger for speciation and/or asexuality (e.g. Otto and Whitton 2000; Hörandl 2023). In this study, populations from which multiple polyploids were collected are limited to locality 2 and 3, making it difficult to infer the reproductive strategies of polyploids of other localities. The polyploids from locality 2 and 3 likely reproduce asexually. The MIG-seq data analyses showed that these populations were composed of genetically identical individuals, and crossing experiments resulted in no fertilization occurring between the polyploids from locality 3. In culture conditions, zoids from the polyploid gametophytic thalli developed into erect thalli or discoid thalli (sporophytic thalli) (data not shown). To infer the life cycle of the polyploids, it is necessary to examine whether the discoidal thalli develop uniocular sporangia.

The presence of both sex chromosomes in polyploids (Hoshino *et al*. 2021a; this study) suggests that the origin of the *Scytosiphon* polyploids is likely a byproduct of the lack of meiosis following fertilization, rather than genome duplication in a single individual. It is unclear how meiosis is avoided. It is possible that being polyploid is adaptive (or that meiosis to haploid is maladaptive), leading to the maintenance of the polyploid state. In land plants and animals, polyploids sometimes exhibit increased resistance against specific stressors, such as pathogens and temperature variation (Lu *et al*. 2016; van de Peer *et al*. 2017; Chauve *et al*. 2023). The distribution of *Scytosiphon* polyploids appears to be biased toward cold regions (Hoshino *et al*. 2021a; this study), suggesting that polyploidy may have adaptive significance to low-temperature environments. The potential for ploidy elevation in *Scytosiphon* to give resistance to environmental stresses, such as low temperatures, needs to be addressed in the future.

For the allopolyploids, which originated in hybrids of *S. promiscuus* and *S. shibazakiorum*, avoiding meiosis is likely advantageous. Given that the *cox*1 haplotypes of the allopolyploids belonged to the *S. promiscuus* lineage and considering maternal inheritance of mitochondria in *Scytosiphon* (Kato *et al*. 2006), the polyploids originated in hybrids between *S. promiscuus* female and *S. shibazakiorum* male. Laboratory crossing experiments also showed that these two species form hybrids only when *S. promiscuus* females and *S. shibazakiorum* males are crossed (Hoshino *et al*. 2018: *S. promiscuus* as species III and *S. shibazakiorum* as species II). The meiospores produced by these hybrid sporophytes are known to have an extremely low survival rate (Hoshino *et al*. 2018), probably due to disrupted meiosis. Meiosis would thus be a dead end for the allopolyploids. It has been pointed out that interspecific hybridization can disrupt meiosis and create opportunities for the selection of asexual cytological mechanisms (Vrijenhoek 1998), such as the production of unreduced gametes/spores, and indeed, many asexual organisms of hybrid origin are known across a wide range of taxa (Simon *et al*. 2003; Hörandl 2023), including seaweeds such as *Ulva* (Cui *et al*. 2018).

Parthenogenetic Amazon populations

The investigation of sex ratio and genetic diversity detected a new Amazon population at locality 20, in addition to the previously reported Amazon populations at locality 17 and 18 (Hoshino *et al*. 2024). The MIG-seq data, in combination

Fig. 4. Results of the *cox*1-based species delimitation analyses. The results of each analysis are shown next to the ultrametric tree. The GMYC results are shown separately for each prior model combination: ^{CR}, coalescent and relaxed model prior; ^{CS}, coalescent and strict clock prior; ^{YR}, Yule and relaxed clock model prior; ^{YS}; Yule and strict clock model prior. Codes are assigned to the putative species inferred by GMYC^{CR} in *S. promiscuus*, *S. shibazakiorum*, and *S. lomentaria*. For comparison, the species boundaries inferred from crossing experiments (Hoshino *et al*. 2018, 2021b; this study) are shown on the right as BSB (biological species boundary). The *cox*1 haplotype from the holotype of *S. promiscuus* is indicated by the arrow.

with the reference genome, also revealed that the Amazon populations exhibit high LD (suppression of recombination of chromosomes). This fact indicates that these Amazon populations did not simply exhibit a temporary female-biased sex ratio at the time of sampling but were in fact populations that have been maintained by parthenogenesis for a long period of time. The SNP-based phylogenetic analysis indicated that the Amazon populations evolved independently twice in *spro2*, which is consistent with our previous phylogenetic analyses based on transcriptome data (Hoshino *et al*. 2024).

In *S. lomentaria*, Amazon populations are reported to be biased toward cold waters (Hoshino *et al*. 2021a). In *spro2*, the number of sampling sites was insufficient to infer the distribution pattern of Amazon populations. However, locality 18 and 20, where Amazon populations were found, are relatively warm regions in Japan, influenced by the warm ocean current. The Amazon populations of *spro2* may have a different distributional pattern from those of *S. lomentaria*. In *S. lomentaria*, it is also reported that, in areas where sexual and Amazon populations are distributed parapatrically, Amazon populations are biased to wave-exposed areas more than sexual populations (Hoshino *et al*. 2021a). It has been speculated that this is because rough waves reduce the efficiency of sexual reproduction (i.e. the encounter of female and male gametes) but have little impact on the efficiency of parthenogenesis (Hoshino *et al*. 2021a). It was probably the case for *spro2* as well. At locality 18–20, sexual and Amazon populations were distributed parapatrically (Fig. 1b). In this area, the sexual population was inside the bay (locality 19), while Amazon populations were outside the bay (locality 18 and 20).

Previous analyses estimated the divergence of the Amazon populations from their sexual ancestors to have occurred approximately 1.5 million years ago in both *S. promiscuus* and *S. lomentaria* (Hoshino *et al*. 2024). However, their origin remains unclear. Interspecies hybridization and/or polyploidy are generally recognized as major triggers of asexuality (Simon *et al*. 2003; Hörandl 2023). Indeed, the asexual polyploids at locality 2 likely originated through interspecies hybridization. In contrast, for the Amazon populations, no evidence of hybridization—such as discordance between nuclear markers associated with asexuality and organellar markers (e.g. mitochondrial introgression)—has been detected (Hoshino *et al*. 2021a; this study). So far, the Amazon populations of *Scytosiphon* consistently exhibit decay of traits considered essential for sexual reproduction, such as sex pheromone production and the ability of zygote formation (e.g. Hoshino *et al*. 2019, 2021a, 2024). These observations have led to the hypothesis that these populations may have transitioned to a parthenogenetic life cycle as a result of the accidental loss of the sexual traits through mutation (Hoshino *et al*. 2024). However, an alternative scenario is also possible: the loss of sexual traits may have occurred after the transition to a parthenogenetic life cycle, once they were no longer necessary (Hoshino *et al*. 2024). As noted above, the Amazon populations have been found in environments that differ from those of their closely related sexual counterparts, which has led to speculation that their origin may be associated with adaptation to these distinct environments.

S. promiscuus species complex

The MIG-seq data revealed that *S. promiscuus* includes two groups (*spro1* and *spro2*), which share few common loci. Crossing experiments showed that these two entities are reproductively isolated, at least at locality 16, where they coexist. This indicates that *spro1* and *spro2* are distinct species. Few common loci between them may imply that their genomes are too differentiated to amplify common loci during library preparation or to map reads of *spro1* individuals to the reference genome, which is based on a *spro2* individual.

*Cox*1-based species delimitation analyses (e.g. GMYC and PTP) have been performed in many studies as an initial step to assess species diversity (Martins *et al*. 2021; Fumo and Sherwood 2023; Neiva *et al*. 2023; Fontana *et al*. 2024). However, among our species delimitation analyses, only GMYC inferred *spro1* and *spro2* as distinct species, although GMYC further delimited *spro1* into at least two species (Sp-G1 and Sp-G3; Fig. 4). Among the individuals used for MIG-seq, only the polyploid asexuals from locality 2 (hybrids of *S. promiscuus* and *S. shibazakiorum*) belonged to Sp-G3. Therefore, based on our results alone, it is difficult to determine whether Sp-G3 and Sp-G1 are distinct species. Most of the *cox*1 sequences belonging to Sp-G3 were reported from North America by McDevit and Saunders (2017), and they include the sequence of the type specimen of *S. promiscuus*. Interestingly, McDevit and Saunders (2017) reported frequent mitochondrial introgression of *S. promiscuus* into other *Scytosiphon* species (*S. shibazakiorum* and *S. lomentaria*) in North America. In Sp-G3, hybridization with other species, similar to what we observed in locality 2, might also have occurred. For a taxonomic revision of the *S. promiscuus* species complex, it is necessary to investigate the nature of Sp-G3 and its relationships with Sp-G1 and Sp-G2 in detail.

Our GMYC inferred multiple putative species also in *S. lomentaria* and *S. shibazakiorum*. *Scytosiphon lomentaria* has been previously examined using MIG-seq data; however, genetic differentiation, such as that observed in *S. promiscuus* in this study, was not detected among the GMYC-based putative species of *S. lomentaria* (Hoshino *et al*. 2021a). At least for *S. lomentaria*, the GMYC of this study seems to overestimate species diversity. Although *cox*1-based species delimitation analyses have been performed for *Scytosiphon* (Hoshino *et al*. 2018, 2021b), we re-performed the analyses with a greater number of *Scytosiphon* haplotypes and different outgroups. As a result, GMYC and PTP inferred more species in *Scytosiphon* compared to the previous studies. At least in *Scytosiphon*, the estimation of some species delimitation appears to be easily changed depending on haplotype/taxon sampling. We believe that MIG-seq can effectively verify the estimation of species delimitation analyses.

Limitation and conclusion of this study

MIG-seq typically yields ~1,000 SNPs (Suyama and Matsuki 2015), which is much fewer than those obtained using other RRS methods such as ddRAD-seq (~100,000) and GRAS-Di (~10,000: Hosoya *et al*. 2019). In this study, the number of SNPs obtained ranged from approximately 670–900 after filtering. Moreover, all individuals, including

haploids and polyploids whose ploidy could not be confirmed as strictly diploid, were treated as diploids for SNP calling. This approach may potentially bias downstream analyses, such as estimates of population genetic diversity, and should therefore be considered with caution.

However, despite the relatively small number of SNPs, this dataset allowed us to obtain preliminary insights on various aspects, including the sex and ploidy of individuals, genetic diversity and reproductive mode of populations, phylogenetic relationships among populations, and the presence of cryptic species. Subsequent validation through crossing experiments and molecular phylogenetic analyses of *cetn*-int2 and *cox1* revealed that *S. promiscuus*, distributed in Japan and its surrounding regions, comprises at least two species, *spro1* and *spro2*. Furthermore, in *spro1*, multiple independent events of polyploidization—likely associated with asexualization—were identified, while in *spro2*, at least two independent emergences of Amazon populations, which are female populations reproducing via parthenogenesis, were detected. *Scytosiphon promiscuus* has been reported from various regions around the world (McDevit and Saunders 2017; Hoshino 2021; Croce *et al*. 2023). This widespread occurrence may be partly explained by its diversity in ploidy and reproductive modes.

ACKNOWLEDGMENTS

We are grateful to Dr. J. Ishigohoka for providing valuable insights and discussions regarding data analyses. We thank Mr. K. Shibazaki and Mrs. K. Shibazaki for their help in sampling at O. Bay, Dr. N. Klochkova, Dr. N. Yotsukura, Dr. T. Abe, and Dr. T. Kawai for their support in sampling in Russia, and the staff of Muroran Marine Station and Akkeshi Marine Station for their support with sampling. This work was supported by JSPS KAKENHI Grant Number JP21570084 and JP19K06817 to K. K., and by Max-Planck-Gesellschaft and JSPS KAKENHI Grant Number 23K19386 to M. Hoshino.

DATA AVAILABILITY STATEMENT

The data that support the findings of this study are openly available in NCBI at https://www.ncbi.nlm.nih.gov.

REFERENCES

Arai, T., Koiwai, K., Nozaki, R. *et al*. 2024. Field survey of the phase and sex ratios of the brown alga *Dictyota dichotoma* (Dictyotales, Phaeophyceae) using sex-specific molecular markers. *Phycol. Res.* **72**: 123–32.

Ardehed, A., Johansson, D., Sundqvist, L. *et al*. 2016. Divergence within and among seaweed siblings (*Fucus vesiculosus* and *F. Radicans*) in the Baltic Sea. *PLoS One* **11**: e0161266.

Barnett, D. W., Garrison, E. K., Quinlan, A. R., Strömberg, M. P. and Marth, G. T. 2011. BamTools: a C++ API and toolkit for analyzing and managing BAM files. *Bioinformatics* **27**: 1691–2.

Barrera-Redondo, J., Lipinska, A. P., Liu, P. *et al*. 2025. Origin and evolutionary trajectories of brown algal sex chromosomes. Nat. Ecol. Evol. (in press). https://doi.org/10.1038/s41559-025-02838-w.

Bolger, A. M., Lohse, M. and Usadel, B. 2014. Trimmomatic: a flexible trimmer for Illumina sequence data. *Bioinformatics* **30**: 2114–20.

Bouckaert, R., Vaughan, T. G., Barido-Sottani, J. *et al*. 2019. BEAST 2.5: an advanced software platform for Bayesian evolutionary analysis. *PLoS Comput. Biol.* **15**: e1006650.

Bradbury, P. J., Zhang, Z., Kroon, D. E., Casstevens, T. M., Ramdoss, Y. and Buckler, E. S. 2007. TASSEL: software for association mapping of complex traits in diverse samples. *Bioinformatics* **23**: 2633–5.

Chang, C. C., Chow, C. C., Tellier, L. C., Vattikuti, S., Purcell, S. M. and Lee, J. J. 2015. Second-generation PLINK: rising to the challenge of larger and richer datasets. *Gigascience* **4**: 7.

Chauve, L., McGarry, A., Butler, L. and McLysaght, A. 2023. Synthetic autotetraploid *Caenorhabditis elegans* resist severe cold stress by escaping cold induced death at the gravid adult stage. bioRxiv. https://doi.org/10.1101/2023.06.28.546823.

Chernomor, O., Von Haeseler, A. and Minh, B. Q. 2016. Terrace aware data structure for Phylogenomic inference from Supermatrices. *Syst. Biol.* **65**: 997–1008.

Couceiro, L., Le Gac, M., Hunsperger, H. M. *et al*. 2015. Evolution and maintenance of haploid-diploid life cycles in natural populations: the case of the marine brown alga *Ectocarpus*. *Evolution* **69**: 1808–22.

Croce, M. E., Hoshino, M., Gauna, M. C., Parodi, E. R. and Kogame, K. 2023. Taxonomic study of *Scytosiphon* (Phaeophyceae) from temperate coasts of Argentina. *J. Phycol.* **59**: 383–401.

Cui, J., Monotilla, A. P., Zhu, W. *et al*. 2018. Taxonomic reassessment of *Ulva prolifera* (Ulvophyceae, Chlorophyta) based on specimens from the type locality and Yellow Sea green tides. *Phycologia* **57**: 692–704.

Danecek, P., Auton, A., Abecasis, G. *et al*. 2011. The variant call format and VCFtools. *Bioinformatics* **27**: 2156–8.

Dorken, M. E. and Eckert, C. G. 2001. Severely reduced sexual reproduction in northern populations of a clonal plant, *Decodon verticillatus* (Lythraceae). *J. Ecol.* **89**: 339–50.

Ellegren, H. 2004. Microsatellites: simple sequences with complex evolution. *Nat. Rev. Genet.* **5**: 435–45.

Evanno, G., Regnaut, S. and Goudet, J. 2005. Detecting the number of clusters of individuals using the software structure : a simulation study. *Mol. Ecol.* **14**: 2611–20.

Fontana, S., Wang, W.-L., Tseng, K.-Y. *et al*. 2024. Seaweed diversification driven by Taiwan's emergence and the Kuroshio current: insights from the cryptic diversity and phylogeography of *Dichotomaria* (Galaxauraceae, Rhodophyta). *Front. Ecol. Evol.* **12**: 1346199.

Francis, R. M. 2017. POPHELPER: an R package and web app to analyse and visualize population structure. *Mol. Ecol. Resour.* **17**: 27–32.

Freitas, S., Parker, D. J., Labédan, M., Dumas, Z. and Schwander, T. 2023. Evidence for cryptic sex in parthenogenetic stick insects of the genus *Timema*. *Proc. R. Soc. B* **290**: 20230404.

Fu, G., Kinoshita, N., Nagasato, C. and Motomura, T. 2014. Fertilization of brown algae: flagellar function in phototaxis and chemotaxis. *In* Sawada, H., Inoue, N. and Iwano, M. (Eds). *Sexual Reproduction in Animals and Plants*. Springer Japan, Tokyo, pp. 359–67.

Fujisawa, T. and Barraclough, T. G. 2013. Delimiting species using single-locus data and the generalized mixed yule coalescent approach: a revised method and evaluation on simulated data sets. *Syst. Biol.* **62**: 707–24.

Fumo, J. T. and Sherwood, A. R. 2023. Phylogeography of *Amansia glomerata* C.Agardh (Ceramiales, Rhodomelaceae) in Hawai'i: a single species with high divergence. *Cryptogam. Algol.* **44**: 85–100.

Guindon, S., Dufayard, J.-F., Lefort, V., Anisimova, M., Hordijk, W. and Gascuel, O. 2010. New algorithms and methods to estimate maximum-likelihood phylogenies: assessing the performance of PhyML 3.0. *Syst. Biol.* **59**: 307–21.

Han, J. W., Klochkova, T. A., Shim, J., Nagasato, C., Motomura, T. and Kim, G. H. 2014. Identification of three proteins involved in fertilization and parthenogenetic development of a brown alga, *Scytosiphon lomentaria*. *Planta* **240**: 1253–67.

Hiraoka, M. and Higa, M. 2016. Novel distribution pattern between coexisting sexual and obligate asexual variants of the true estuarine macroalga *Ulva prolifera*. *Ecol. Evol.* **6**: 3658–71.

Hiraoka, M., Shimada, S., Ohno, M. and Serisawa, Y. 2003. Asexual life history by quadriflagellate swarmers of *Ulva spinulosa* (Ulvales, Ulvophyceae). *Phycol. Res.* **51**: 29–34.

Hörandl, E. 2023. Geographical parthenogenesis in alpine and arctic plants. *Plants* **12**: 844.

Hoshino, M. 2021. Brown algal parthenogenesis in the field. *Jpn. J. Phycol. (Sôrui)* **69**: 95–101.

Hoshino, M., Cossard, G., Haas, F. B. *et al*. 2024. Parallel loss of sexual reproduction in field populations of a brown alga sheds light on the mechanisms underlying the emergence of asexuality. *Nat. Ecol. Evol.* **8**: 1946.

Hoshino, M., Hiruta, S. F., Croce, M. E. *et al*. 2021a. Geographical parthenogenesis in the brown alga *Scytosiphon lomentaria* (Scytosiphonaceae): Sexuals in warm waters and parthenogens in cold waters. *Mol. Ecol.* **30**: 5814–30.

Hoshino, M., Ino, C., Kitayama, T. and Kogame, K. 2020. Integrative systematics approaches revealed that the rare red alga *Schimmelmannia* (Shimmelmanniaceae, Acrosymphytales) from Japan is a new species: the description of *S. Benzaiteniana* sp. nov. *Phycol. Res.* **68**: 290–7.

Hoshino, M., Ishikawa, S. and Kogame, K. 2018. Concordance between DNA-based species boundaries and reproductive isolating barriers in the *Scytosiphon lomentaria* species complex (Ectocarpales, Phaeophyceae). *Phycologia* **57**: 232–42.

Hoshino, M., Okino, T. and Kogame, K. 2019. Parthenogenetic female populations in the brown alga *Scytosiphon lomentaria* (Scytosiphonaceae, Ectocarpales): decay of a sexual trait and acquisition of asexual traits. *J. Phycol.* **55**: 204–13.

Hoshino, M., Tanaka, A., Kamiya, M., Uwai, S., Hiraoka, M. and Kogame, K. 2021b. Systematics, distribution, and sexual compatibility of six *Scytosiphon* species (Scytosiphonaceae, Phaeophyceae) from Japan and the description of four new species. *J. Phycol.* **57**: 416–34.

Hosoya, S., Hirase, S., Kikuchi, K. *et al*. 2019. Random PCR-based genotyping by sequencing technology GRAS-Di (genotyping by random amplicon sequencing, direct) reveals genetic structure of mangrove fishes. *Mol. Ecol. Resour.* **19**: 1153–63.

Kalyaanamoorthy, S., Minh, B. Q., Wong, T. K. F., Von Haeseler, A. and Jermiin, L. S. 2017. ModelFinder: fast model selection for accurate phylogenetic estimates. *Nat. Methods* **14**: 587–9.

Kamiya, M., Saba, E., West, J. A. and Lane, C. 2017. Marginal distribution and high heterozygosity of asexual *Caloglossa vieillardii* (Delesseriaceae, Rhodophyta) along the Australian coasts. *J. Phycol.* **53**: 1283–93.

Kato, Y., Kogame, K., Nagasato, C. and Motomura, T. 2006. Inheritance of mitochondrial and chloroplast genomes in the isogamous brown alga *Scytosiphon lomentaria* (Phaeophyceae). *Phycol. Res.* **54**: 65–71.

Katoh, K. 2002. MAFFT: a novel method for rapid multiple sequence alignment based on fast Fourier transform. *Nucleic Acids Res.* **30**: 3059–66.

Katoh, K. and Standley, D. M. 2013. MAFFT multiple sequence alignment software version 7: improvements in performance and usability. *Mol. Biol. Evol.* **30**: 772–80.

Kogame, K., Ishikawa, S., Yamauchi, K., Uwai, S., Kurihara, A. and Masuda, M. 2015. Delimitation of cryptic species of the *Scytosiphon lomentaria* complex (Scytosiphonaceae, Phaeophyceae) in Japan, based on mitochondrial and nuclear molecular markers. *Phycol. Res.* **63**: 167–77.

Krueger-Hadfield, S. A. 2024. Let's talk about sex: why reproductive systems matter for understanding algae. *J. Phycol.* **60**: 581–97.

Krueger-Hadfield, S. A., Flanagan, B. A., Godfroy, O. *et al*. 2021. Using RAD-seq to develop sex-linked markers in a haplodiplontic alga. *J. Phycol.* **57**: 279–94.

Kumer, S., Stecher, G. and Tamura, K. 2016. MEGA7: molecular evolutionary genetics analysis version 7.0 for bigger datasets. *Mol. Biol. Evol.* **33**: 1870–4.

Landan, G. and Graur, D. 2008. Local reliability measures from sets of co-optimal multiple sequence alignments. *Pac. Symp. Biocomput.* **2008**: 15–24.

Leliaert, F., Verbruggen, H., Vanormelingen, P. *et al*. 2014. DNA-based species delimitation in algae. *Eur. J. Phycol.* **49**: 179–96.

Li, H. and Durbin, R. 2009. Fast and accurate short read alignment with burrows–wheeler transform. *Bioinformatics* **25**: 1754–60.

Li, H., Handsaker, B., Wysoker, A. *et al*. 2009. The sequence alignment/map format and SAMtools. *Bioinformatics* **25**: 2078–9.

Li, W. and Godzik, A. 2006. Cd-hit: a fast program for clustering and comparing large sets of protein or nucleotide sequences. *Bioinformatics* **22**: 1658–9.

Lipinska, A. P., Ahmed, S., Peters, A. F., Faugeron, S., Cock, J. M. and Coelho, S. M. 2015. Development of PCR-based markers to determine the sex of kelps. *PLoS One* **10**: e0140535.

Lischer, H. E. L. and Excoffier, L. 2012. PGDSpider: an automated data conversion tool for connecting population genetics and genomics programs. *Bioinformatics* **28**: 298–9.

Lu, Y.-J., Swamy, K. B. S. and Leu, J.-Y. 2016. Experimental evolution reveals interplay between Sch9 and polyploid stability in yeast. *PLoS Genet.* **12**: e1006409.

Martins, N. T., Gurgel, C. F. D., Spokes, T. M. and Cassano, V. 2021. *Colpomenia* species from south and south-eastern Australia (Ectocarpales, Phaeophyceae): a DNA barcoding approach. *Aust. Syst. Bot.* **34**: 587–94.

McDevit, D. C. and Saunders, G. W. 2017. A molecular investigation of Canadian Scytosiphonaceae (Phaeophyceae) including descriptions of *Planosiphon* gen. Nov. and *Scytosiphon promiscuus* sp. nov. *Botany* **95**: 653–71.

Meirmans, P. G. 2020. GENODIVE version 3.0: easy-to-use software for the analysis of genetic data of diploids and polyploids. *Mol. Ecol. Resour.* **20**: 1126–31.

Meirmans, P. G. and Van Tienderen, P. H. 2004. Genotype and genodive: two programs for the analysis of genetic diversity of asexual organisms. *Mol. Ecol. Notes* **4**: 792–4.

Minh, B. Q., Schmidt, H. A., Chernomor, O. *et al*. 2020. IQ-TREE 2: new models and efficient methods for phylogenetic inference in the genomic era. *Mol.Biol. Evol.* **37**: 1530–4.

Müller, D. G. 1977. Sexual reproduction in British *Ectocarpus siliculosus* (Phaeophyta). *Brit. Phycol. J.* **12**: 131–6.

Nei, M. 1987. *Molecular Evolutionary Genetics*. Columbia University Press, New York.

Neiva, J., Bermejo, R., Medrano, A. *et al*. 2023. DNA barcoding reveals cryptic diversity, taxonomic conflicts and novel biogeographical insights in *Cystoseira* s.l. (Phaeophyceae). *Eur. J. Phycol.* **58**: 351–75.

Neiva, J., Serrão, E. A., Anderson, L. *et al*. 2017. Cryptic diversity, geographical endemism and allopolyploidy in NE Pacific seaweeds. *BMC Evol. Biol.* **17**: 30.

Otto, S. P. and Whitton, J. 2000. Polyploid incidence and evolution. *Annu. Rev. Genet.* **34**: 401–37.

Penn, O., Privman, E., Ashkenazy, H., Landan, G., Graur, D. and Pupko, T. 2010. GUIDANCE: a web server for assessing alignment confidence scores. *Nucleic Acids Res.* **38**: W23–8.

Peters, A. F. 1987. Reproduction and sexuality in the Chordariales (Phaeophyceae). A review of culture studies. *In* Chapman, D. J. and Round, F. E. (Eds). *Progress in Phycological Research*. Biopress Ltd., Amsterdam, pp. 223–63.

Peterson, B. K., Weber, J. N., Kay, E. H., Fisher, H. S. and Hoekstra, H. E. 2012. Double digest RADseq: an inexpensive

method for de novo SNP discovery and genotyping in nodel and non-model species. *PLoS One* **7**: e37135.
Pons, J., Barraclough, T. G., Gomez-Zurita, J. *et al*. 2006. Sequence-based species delimitation for the DNA taxonomy of undescribed insects. *Syst. Biol.* **55**: 595–609.
Pritchard, J. K., Stephens, M. and Donnelly, P. 2000. Inference of population structure using multilocus genotype data. *Genetics* **155**: 945–59.
Puillandre, N., Brouillet, S. and Achaz, G. 2021. ASAP: assemble species by automatic partitioning. *Mol. Ecol. Resour.* **21**: 609–20.
Rochette, N. C., Rivera-Colón, A. G. and Catchen, J. M. 2019. Stacks 2: analytical methods for paired-end sequencing improve RADseq-based population genomics. *Mol. Ecol.* **28**: 4737–54.
Sela, I., Ashkenazy, H., Katoh, K. and Pupko, T. 2015. GUIDANCE2: accurate detection of unreliable alignment regions accounting for the uncertainty of multiple parameters. *Nucleic Acids Res.* **43**: W7–W14.
Simon, J.-C., Delmotte, F., Rispe, C. and Crease, T. 2003. Phylogenetic relationships between parthenogens and their sexual relatives: the possible routes to parthenogens in animals. *Biol. J. Linn. Soc.* **79**: 151–63.
Sousa, F., Neiva, J., Martins, N. *et al*. 2019. Increased evolutionary rates and conserved transcriptional response following allopolyploidization in brown algae. *Evolution* **73**: 59–72.
Suyama, Y. and Matsuki, Y. 2015. MIG-seq: an effective PCR-based method for genome-wide single-nucleotide polymorphism genotyping using the next-generation sequencing platform. *Sci. Rep.* **5**: 16963.
Tatewaki, M. 1966. Formation of a crustaceous sporophyte with unilocular sporangia in *Scytosiphon lomentaria*. *Phycologia* **6**: 62–6.
Untergasser, A., Cutcutache, I., Koressaar, T. *et al*. 2012. Primer3—new capabilities and interfaces. *Nucleic Acids Res.* **40**: e115.
van de Peer, Y., Mizrachi, E. and Marchal, K. 2017. The evolutionary significance of polyploidy. *Nat. Rev. Genet.* **18**: 411–24.
Vences, M., Miralles, A., Brouillet, S. *et al*. 2021. iTaxoTools 0.1: Kickstarting a specimen-based software toolkit for taxonomists. *Megataxa* **6**: 77–92.
Vrijenhoek, R. C. 1998. Animal clones and diversity: are natural clones generalist of specialists? *Bioscience* **48**: 617–28.
West, J. A. and Zuccarello, G. C. 1999. Biogeography of sexual and asexual populations in *Bostrychia moritziana* (Rhodomelaceae, Rhodophyta). *Phycol. Res.* **47**: 115–23.
Zhang, J., Kapli, P., Pavlidis, P. and Stamatakis, A. 2013. A general species delimitation method with applications to phylogenetic placements. *Bioinformatics* **29**: 2869–76.
Zupan, J. R. and West, J. A. 1988. Geographic variation in the life history of *Mastocarpus papillatus* (Rhodophyta). *J. Phycol.* **24**: 223–9.

SUPPORTING INFORMATION

Additional Supporting Information may be found in the online version of this article at the publisher's web-site:

Figure S1. Venn diagram showing common and unique SNPs of the SNP datasets.

Figure S2. Electrophoresis pattern of PCR-based sex marker amplicons in female and male gametophytes.

Figure S3. Plots of the estimated probability of data for each *K*. (A) Estimated log probability of data of runs over increasing values of *K*. (B) ΔK calculated by the Evanno *et al*. (2005) method over values of *K*.

Table S1. Sample information.

Table S2. Primers of candidate sex markers.

Table S3. Fertilization rate of intra- and interspecies crossing of *spro1* and *spro2* at locality 16.

Movie S1. Movie of crossing experiment between *spro1* female (Koinoura150323-11) and *spro2* male (Koinoura150323-14).